Experimental Study of Wave Occlusion on Falling Films in a Vertical Pipe

Eric K. Dao and Vemuri Balakotaiah
Dept. of Chemical Engineering, University of Houston, Houston, TX 77204

Experiments were conducted to study wave occlusion on falling films in a vertical pipe with aqueous solutions of glycerine with viscosities from 0.022 to 1.25 kg/(m·s). Pipe diameters were varied from 0.00635 to 0.015875 m. For each case, the critical liquid flow rate was determined at which the free falling wavy annular flow transforms into slug flow due to wave occlusion. The experimental results are correlated in terms of the liquid Reynolds number at occlusion ($Re_{LS} = 4q/\pi\nu D$) and two dimensionless groups influencing the transition: the Kapitza number $Ka = \sigma/[(\nu g)^{1/3}\mu]$, and the Bond number $Bo = \rho g D^2/\sigma$. The annular-slug transition correlation was $Re_{LS} = 0.062\ Ka^{4/3} Bo^{2/3}$ and valid in the range $0.1 < Re_{LS} < 200$, $0.2 < Ka < 55$ and $7 < Bo < 50$. Experimental results were compared to related published results, and the experimental correlation is explained qualitatively.

Introduction

Free falling wavy liquid films occur in many chemical and industrial processes such as condensers and reboilers, falling film exchangers (liquid coolers and condensers, evaporators, and absorbers), gas-liquid reactors, and thin film coating operations. To understand such processes better and to design them economically and effectively, numerous investigations have been carried out over the past several decades on wavy films (Hewitt and Whalley, 1989). Experimentally, it is observed that the interface of a liquid film falling down a vertical pipe is a complex wavy surface. Most design procedures assume a smooth interface for heat and mass transfer. As a result, these design methods have been approximate and overly conservative. The wavy interface can increase the rate of heat and mass transfer by 200%-300% (Dukler, 1977-1978). However, when wave occlusion occurs, the gas-liquid interfacial area reduces and affects the operating conditions of these processes. For liquids with high viscosity, the slug-annular transition is very sensitive to changes in the flow rate. To keep a process operating in an annular flow regime, the transition boundary between wavy annular flow and slug flow needs to be understood.

An understanding of the mechanism of the annular-slug transition is also important in developing flow pattern maps for two-phase-gas-liquid flows. It is well known that there are three major flow regimes for free falling liquid in a vertical pipe, namely, bubble, slug, and annular flow. The liquidsurface in annular flow is always covered with a complex wave pattern. Two different types of waves have been observed (Dukler 1977-1978). The first type, called ''ripple'' waves, occur at all liquid flow rates. They are of high frequency and small amplitude, and appear to rapidly lose their identity on passing downstream. These waves are not axially symmetric. At high liquid-flow rate, ''disturbance'' or ''roll'' waves are observed. These waves have far greater amplitude than the ripples. They are axially symmetric (for low Reynolds numbers and Kapitza numbers) and coherent, and the passage of these waves downstream can be readily followed. As the liquid flow rate increases, the amplitude of the roll waves increases. When the wave amplitudes are large enough, wave occlusion will occur, as shown in Figure 1. Most of the previous work on two-phase gas-liquid flows in vertical pipes dealt with determining the flow pattern maps for air-water systems (Dukler and Taitel, 1986). Systematic studies of wave occlusion on falling films in vertical pipes are currently lacking.

This work is focused on wave occlusion on falling films in a vertical pipe. The main objective of this work is to determine experimentally the critical flow rate at which wave occlusion occurs as a function of the liquid physical properties and pipe diameter.

Correspondence concerning this article should be addressed to V. Balakotaiah.

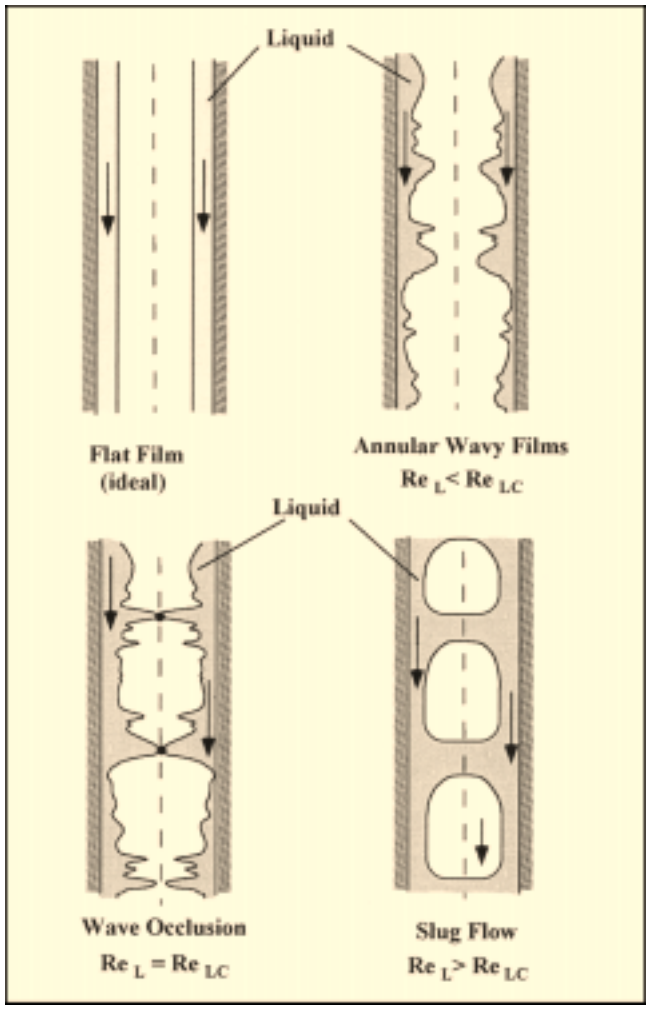

Figure 1. Wave occlusion and annular-slug flow transition in vertical pipes.

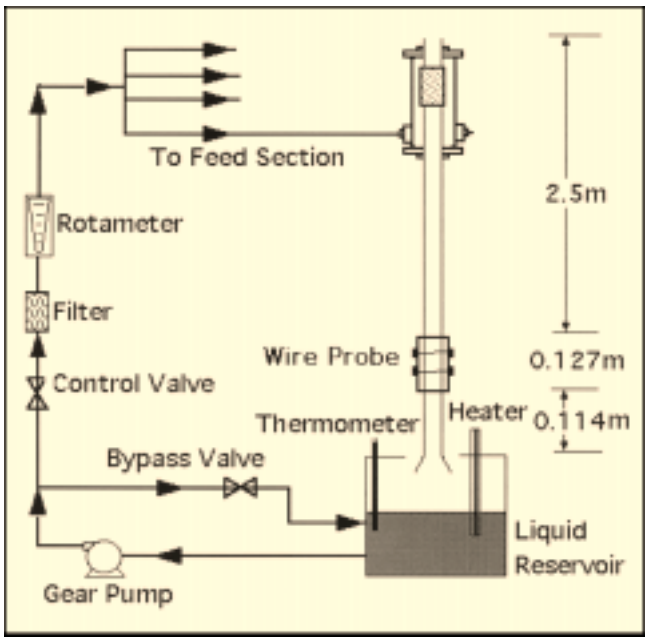

Figure 2. Flow loop used in the experiments for solutions with viscosity from 22 to 90 cp.

Experiments on Wave Occlusion in a Vertical Pipe

The experiments were conducted using liquid glycerine and water solutions with various concentrations and temperatures close to the ambient value. The solution viscosities varied from 0.022 to 1.25 kg/(m·s), densities from 1,170 to 1,260 kg/m^3, and surface tensions from 0.064 to 0.068 kg/s^2. Four different pipe diameters in the range 0.00635 m (0.25 in.) to 0.015875 m (0.625 in.) were used. The flow loop used in the experiments is shown in Figure 2 for glycerine solutions with viscosity in the range 0.022 to 0.0893 kg/(m·s).

The test section is made of two segments of Plexiglas tube with an overall length of 2.74 m. It is equipped with two conductance probes at 2.54 m down the pipe to detect the wave occlusion. The two probes, 0.0508 m (2.0 in.) apart, are used to estimate the speed of a particular wave as it travels from one probe to another. Each conductance probe in the test section is made of two parallel wires with 2.5×10^{-3} m spacing. The wires are 7.6×10^{-5} m in diameter and made of Platinum-Rhodium alloy (containing 13% Rhodium for better strength). The wire probes measured the voidage of the liquid film as its traveled across the parallel pairs of wires. The signal is monitored and converted from analog to digital using the data acquisition devices. The output voltage is connected to an oscilloscope to display the waveform on the screen.

The feed section is also made of Plexiglas. The feed section was designed in order to introduce the liquid smoothly and uniformly onto the inside wall of the tube. There are 108 holes (3×10^{-3} m in diameter) on the tube at the feed section and a differential screen (made of several sets of layers) to produce a falling film with uniform thickness at the entrance section. Liquid glycerine solution is pumped from the reservoir through the filter and rotameter to the feed section. Under pumping pressure, the liquid in the feed section rises up, goes through the screen, enters the test section, and falls by gravity. After a short distance, the liquid layer forms a wavy film. As this wavy film travels down the pipe, the amplitude of the wave increases and reaches an asymptotic value. Beyond a certain flow rate, this asymptotic value exceeds the pipe radius and the wave bridges and forms a liquid slug traveling down the pipe. The experiments focused on the location of the occlusion point about 180 to 200 times the pipe diameter in order for the waves to be well developed.

Experimental procedures

The liquid solution was prepared by mixing glycerine (99.5% pure) with distilled water. Table salt was added (1.67 kg NaCl per m^3 solution) to increase the liquid conductivity, and the solution was brought to about 24°C using a liquid heater. The liquid was mixed carefully before taking the temperature to avoid temperature gradients in the liquid. The liquid was then circulated in the loop by pumping for about 5 min. To detect wave occlusion, the signal was recorded when the tube was filled with the liquid. This signal displayed a

straight line on the oscilloscope. The wave occlusion was then detected by varying the flow rate until the peak of the signal touched the horizontal line representing the bridging of the liquid. The liquid flow rate was varied from annular to slug and vice versa in small amounts to determine the flow rate at which occlusion occurred. The experiment was repeated several times until the transition flow rate was reproduced. The temperature was checked during the experiment to make sure that it did not vary by more than a degree. The flow rate at occlusion was measured manually by bypassing the liquid before it went to the reservoir. After running an experiment, the density and viscosity of the liquid was measured with a Fenske viscometer. The liquid was kept at the same temperature as the operating temperature of the experiment to eliminate the variation of viscosity with temperature.

For glycerine solutions with viscosity higher than 0.09 kg/(m·s), the wire probes cannot be used to detect the wave signals since the conductivity of the liquid glycerine is very weak at high concentration. Since the wave velocity is small, wave occlusion can be detected visually. A different feed section is used to introduce the liquid smoothly onto the inside wall of the tube.

The sufficiency of the flow development length (from feed to the location where film thickness was measured to identify occlusion) was also verified by determining how the occlusion point moved as the flow rate was increased beyond the critical value. For viscous solutions ($\mu > 0.09$ kg/(m·s)), the occlusion point could be seen visually and was found to be very sensitive to the flow rate. Even small increases (of the order of 1 to 2%) in the flow rate (beyond the critical value) were sufficient to move the occlusion point upstream substantially (0.3 to 0.6 m).

Correlation and Analysis of Experimental Data

In our present system, the significant variables influencing the critical flow rate or superficial velocity (u_{LS}) are ρ, μ, σ, D, and g. Here, ρ and μ are the liquid density and viscosity, σ is the surface tension of the liquid, D is diameter of the tube, and g is the gravitational acceleration. Using D, ρ, and μ as the core variables, we identify three independent dimensionless groups: $Re_{LS} = \rho u_{LS} D/\mu$, $Su = \sigma D\rho/\mu^2$, and $Ga = gD^3/\nu^2$, where Re_{LS} is the liquid Reynolds number based on the superficial velocity, Su is the Suratman number, and Ga is the Galileo number. This dimensional analysis shows that the dimensionless critical flow rate (or the liquid Reynolds number) at which wave occlusion occurs can be correlated by the other two dimensionless groups, which are the Suratman number and Galileo number $Re_{LS} = f(Su, Ga)$. Since we varied mainly the viscosity and the pipe diameter, these two variables can be isolated from the Suratman number and the Galileo number. The resulting two dimensionless groups are the Kapitza number $Ka = Su/Ga^{1/3} = \sigma/[(\nu g)^{1/3}\mu]$ and the Bond number $Bo = Ga/Su = \rho g D^2/\sigma$. Hence, the critical liquid Reynolds number at which wave occlusion occurs can also be expressed as a function of the Kapitza and Bond numbers $Re_{LS} = f(Ka, Bo)$.

The experimental results are tabulated in Table 1, and Table 2 shows values of various dimensionless groups. Here, the superficial velocity is given by $u_{LS} = 4q/\pi D^2$. The expression for the liquid Reynolds number as a function of flow rate is $Re_{LS} = 4q/\pi\nu D$. Other dimensionless groups listed in Table 2 include the product Ka^2Bo and the Capillary number $Ca = Re_{LS}/Su = \mu u_{LS}/\sigma$. The surface tensions were approximated using data for aqueous glycerine solutions at 18°C from the CRC Handbook (1978).

The results show that the critical liquid Reynolds number for occlusion decreases when the viscosity of the glycerine solution increases. The maximum error estimated for experimental densities is about 1.0%. Likewise, the estimated errors for the viscosities and the flow rates are less than 3.0%. The critical Reynolds number was plotted vs. the Kapitza number in a log-log graph to determine the dependence of

Table 1. Experimental Data on Wave Occlusion

Variable Est. Err. % gly. Data No.	 ±3	D(m) $\pm 10^{-5}$	T(°C) ±0.5°C	μ(kg/m·s) ±3%	ρ(kg/m^3) ±10	σ(kg/s^2) ±0.0005	q(kg/s) ±3%
1	70	0.0127	25	0.022	1,177.8	0.0678	0.04572
2	73	0.0127	25	0.026	1,182.3	0.0674	0.03445
3	75	0.0127	25	0.035	1,190.8	0.0672	0.02129
4	83	0.0127	25	0.089	1,202.0	0.0661	0.00514
5	84	0.0127	19.4	0.140	1,218.3	0.066	0.00493
6	90	0.0127	25	0.226	1,218.8	0.065	0.00410
7	92	0.0127	25	0.391	1,236.7	0.645	0.00442
8	90	0.0127	19.2	0.440	1,234.0	0.065	0.00454
9	95	0.0127	19.4	1.252	1,248.6	0.064	0.00224
10	90	0.00635	19.4	0.185	1,234.7	0.065	0.00073
11	90	0.00953	19.4	0.185	1,234.7	0.065	0.00217
12	90	0.0127	19.4	0.185	1,234.7	0.065	0.00509
13	89	0.00635	25	0.167	1,223.9	0.065	0.00043
14	89	0.00953	25	0.167	1,223.9	0.065	0.00225
15	89	0.0127	25	0.167	1,223.9	0.065	0.00526
16	83	0.00953	26.1	0.125	1,214.7	0.0661	0.00237
17	83	0.0127	26.1	0.125	1,214.7	0.0661	0.00593
18	83	0.01588	26.1	0.125	1,214.7	0.0661	0.01013
19	80	0.00953	19.4	0.107	1,220.0	0.066	0.00240
20	99	0.00953	19.4	1.049	1,260.7	0.064	0.00078

Table 2. Values of the Various Dimensionless Groups at the Annular-Slug Transition Boundary

Expt. No.	Re_{LS}	Ga	Su	Ka	Bo	Ca	Ka^2Bo
1	207.16	56,945.1	2,071.8	53.85	27.5	0.100	79,705.9
2	132.79	41,519.8	1,495.9	43.20	27.8	0.089	51,799.9
3	60.17	22,645.7	807.7	28.55	28.0	0.074	22,850.9
4	5.77	3,639.1	126.5	8.22	28.8	0.046	1,945.40
5	3.54	1,528.8	52.3	4.54	29.2	0.068	602.98
6	1.82	586.9	19.8	2.36	29.7	0.092	165.64
7	1.13	201.3	6.6	1.13	30.3	0.171	38.88
8	1.03	158.0	5.3	0.97	30.0	0.196	28.44
9	0.18	20.0	0.6	0.24	30.9	0.277	1.76
10	0.79	112.0	14.9	3.09	7.5	0.053	71.85
11	1.57	378.0	22.4	3.09	16.9	0.070	161.67
12	2.76	896.0	29.8	3.09	30.1	0.093	287.42
13	0.52	134.3	18.0	3.52	7.4	0.029	92.34
14	1.80	453.3	27.0	3.52	16.8	0.066	207.76
15	3.15	1,074.4	36.1	3.52	29.8	0.087	369.36
16	2.53	795.7	48.6	5.25	16.4	0.052	450.81
17	4.74	1,886.1	64.9	5.25	29.1	0.073	801.44
18	6.48	3,683.8	81.1	5.25	45.4	0.080	1,252.25
19	3.01	1,108.9	67.4	6.51	16.5	0.045	697.67
20	0.10	12.2	0.7	0.30	17.5	0.142	1.61

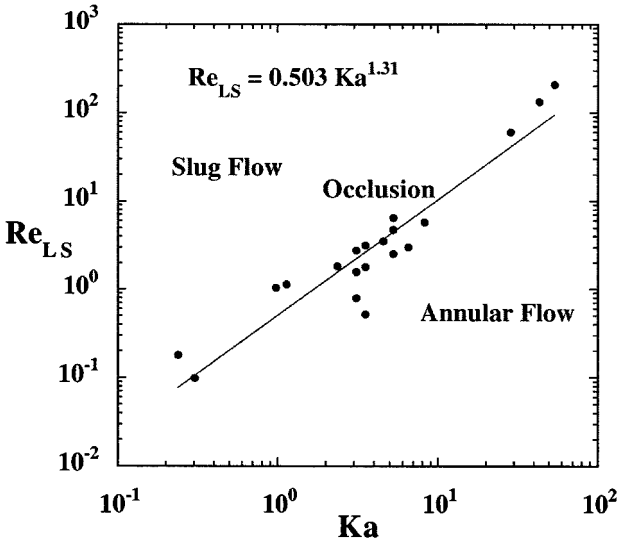

Figure 3. Dependence of the critical flow rate (Reynolds number) at occlusion on the Kapitza number.

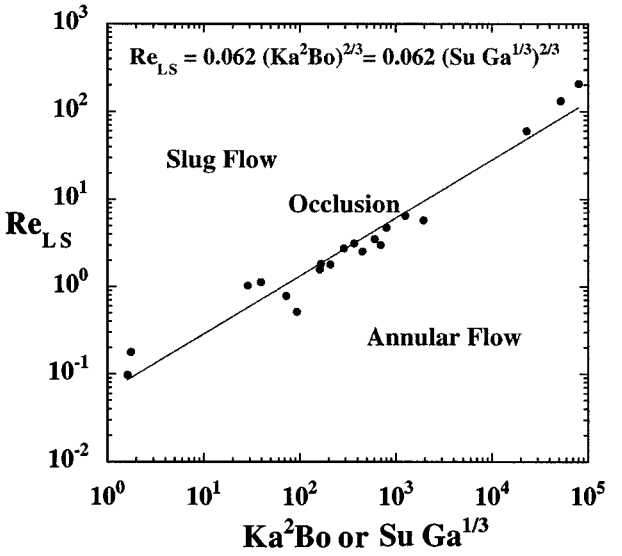

Figure 5. Dependence of the critical flow rate (Reynolds number) at occlusion on the Kapitza and Bond (or Suratman and Galileo) numbers for all experiments.

the flow rate at occlusion on the liquid viscosity. This plot shown in Figure 3 gives a straight line with a slope of 1.31. To examine the dependence of critical flow rate on the tube diameter, experiments were conducted using the same liquid glycerine solution, but with different tube diameters. A plot of critical Re_{LS} vs. Bo for the two data sets gave a straight line with slopes of 0.71 and 0.72, respectively (Figure 4). Since we used different diameter tubes, the flow rates at occlusion from Figure 5 were based on approximately the same length (distance from the inlet end to occlusion point) to diameter ratio. To get the final correlation between Re_{LS} and the Kapitza and Bond numbers, we have plotted the critical Reynolds number vs. the product Ka^2Bo in Figure 5. The 20 different experiments with various fluids and tube diameters covered approximately five orders of magnitude of the product Ka^2Bo. The data shown on a logarithmic scale in Figure 6 are well correlated by a straight line with a slope of 2/3. Since $SuGa^{1/3} = Ka^2Bo$, a plot of Re_{LS} vs. $SuGa^{1/3}$ also gives a straight line with an identical slope (Figure 5). Thus, our final correlation between the critical liquid Reynolds number, at which occlusion occurs, and the dimensionless groups representing the physical properties of the liquid and the pipe

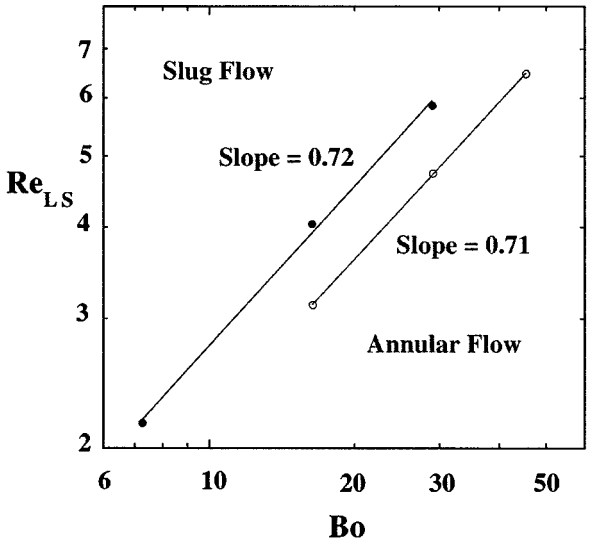

Figure 4. Dependence of the critical flow rate (Reynolds number) at occlusion on the Bond number.

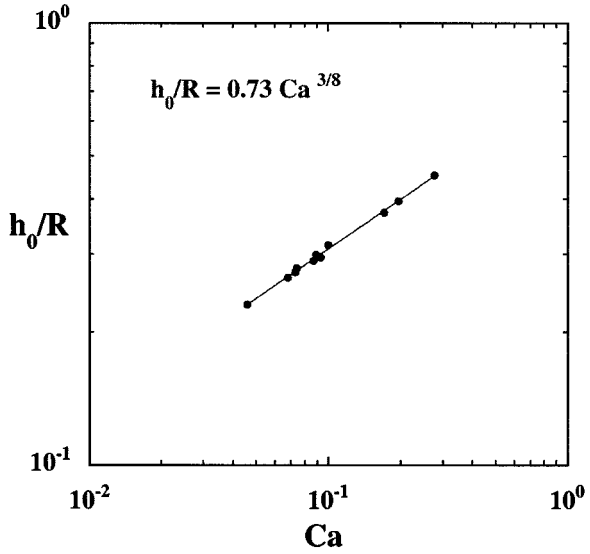

Figure 6. Dependence of scaled average film thickness at occlusion on the Capillary number.

diameter was found to be

$$Re_{LS} = 0.062\, Ka^{4/3} Bo^{2/3} \tag{1a}$$

$$= 0.062\, Ka^{2/3} Ga^{4/9} \tag{1b}$$

$$= 0.062\, Su^{2/3} Ga^{2/9}, \tag{1c}$$

where

$$Ka^{4/3} Bo^{2/3} = Ka^{2/3} Ga^{4/9} = Su^{2/3} Ga^{2/9} = \frac{\sigma^{2/3} \rho^{10/9} D^{4/3} g^{2/9}}{\mu^{16/9}}. \tag{2}$$

This correlation is valid in the range of our experiments $0.1 < Re_{LS} < 200$, $0.2 < Ka < 55$, $7 < Bo < 50$, $0.6 < Su < 2070$ and $12 < Ga < 57000$. The above correlation may be rewritten in terms of the critical volumetric flow rate at occlusion as a function of the liquid properties, the pipe diameter, and the gravitational acceleration as

$$q = 0.048 \frac{\sigma^{2/3} \rho^{1/9} g^{2/9} D^{7/3}}{\mu^{7/9}}. \tag{3}$$

Equations 1a and 3 summarize the main result of this work.

Discussion

We now give a qualitative explanation of our experimental correlation Eq. 1. For an ideal free falling flat film, assuming axisymmetric flow with zero pressure gradient along the vertical axis, we have the relation

$$Re_{LS} = \frac{\rho^2 g D^3}{32 \mu^2} f(h_0) = \frac{Ga}{32} f(h_0), \tag{4}$$

where

$$f(h) = \left[1 - 4\left(1 - \frac{h}{R}\right)^2 + 3\left(1 - \frac{h}{R}\right)^4 - 4\left(1 - \frac{h}{R}\right)^4 \ln\left(1 - \frac{h}{R}\right) \right], \tag{5}$$

and h_0 is the flat film thickness. (This relation is obtained by integrating the z-momentum balance to obtain the velocity profile and, hence, the flow rate of the ideal flat film in a vertical pipe. It reduces to the Hagen-Poiseuille relation when $h = R$.) Since $f(R) = 1$, Eq. 4 shows that, if there are no waves on the film, then the critical Reynolds number at occlusion is equal to 1/32 times the Galileo number ($Re_{LS} = Ga/32$). Intuitively, we expect that the presence of waves reduces the critical flow rate to a fraction of this value. Since the wave amplitude depends on the surface tension (as well as other variables), based on dimensional arguments, we can write

$$\frac{h_{\max}}{h_0} - 1 = F(Re_{LS}, Ka), \tag{6}$$

where $h_{\max}$ is the maximum wave amplitude (with $h_{\max} = R$ at occlusion) and h_0 is defined by Eq. 4. We do not include the dependence on Ga on the righthand of Eq. 6, since for any fixed h_0, Re_{LS}, and Ga are related by Eq. 4. We note that the unknown function F should be decreasing as Ka is increased (since waves are suppressed for the higher values of σ) and must approach zero for $Ka \to \infty$. Comparing Eqs. 4 and 1 shows that the presence of waves reduces the exponent on Ga. This comparison also shows that the critical flow rate has a 2/3 power dependence on the surface tension. The numerical values in Table 2 indicate that the critical Reynolds number at occlusion is approximately 3 to 20 times smaller than the value in the absence of waves ($Ga/32$).

Determining the exact form of the function F requires an analysis of the full Navier-Stokes equations in the nonlinear regime. Since this problem has not been attempted in the literature for cylindrical coordinates, we consider the analogous problem in rectangular coordinates. Nguyen and Balakotaiah (1999) analyzed the two-dimensional film flow equations using the bifurcation theory and showed that the maximum amplitude of any wave on a free falling film on a vertical wall is given by

$$\frac{h_{\max}}{h_0} - 1 = 0.132\, Re^{5/3} Ka^{-1}, \tag{7}$$

where h_0 is the flat (Nusselt) film thickness and Re is the film Reynolds number ($Re = 4\Gamma/\nu$, Γ is the flow rate per unit width, $\Gamma = q/\pi D$ for a circular pipe). The above analytical result (which was also confirmed experimentally by Nguyen and Balakotaiah (1999) in the range $h_{\max} \le 2h_0$ and valid for Re values of order 100 or less) may be used to determine the critical flow rate at occlusion for a vertically falling film between two parallel plates. For plates separated by distance 2h and flat film thickness of h_N, we have

$$h_{\max} = h, \quad Re_{LS} = \frac{4}{3} \frac{g h_0^3}{\nu^2}, \quad Ga = \frac{g(2h)^3}{\nu^2}, \tag{8a}$$

and Eq. 4 is modified to

$$Re_{LS} = \frac{Ga}{6} \left(\frac{h_0}{h} \right)^3. \tag{8b}$$

Combining Eqs. 7 and 8, we get

$$\left(\frac{Ga}{6 Re_{LS}} \right)^{1/3} - 1 = 0.132\, Re_{LS}^{5/3} Ka^{-1}. \tag{9}$$

When the wave amplitude is much larger compared to the flat film thickness, we can ignore the second term on the left-hand side of Eq. 9 and rearrange it as

$$Re_{LS} = 2.04\, Ka^{1/2} Ga^{1/6}. \tag{10}$$

At the other limit in which the wave amplitude is much smaller than the flat film thickness, Eq. 9 may be simplified to

$$Re_{LS} = \frac{Ga/6}{[1+0.02\,Ga^{5/3}\,Ka^{-1}]}. \qquad (11)$$

When h_{max} and h_0 are of the same order of magnitude, Eq. 9 defines an implicit relation between Re_{LS}, Ga, and Ka. Comparing Eqs. 10 and 11 shows that the presence of the waves modifies the dependence of Re_{LS} on Ga from a linear to a weaker dependence with an exponent of 1/6. The exponent on Ga in our correlation falls within this range. Similarly, Re_{LS} depends on Ka with an exponent that varies between zero and 0.5. However, our experiments show a 2/3 power dependence. We believe that this difference may be due to a curvature effect in the pipe (that is, for the same Re_{LS} and Ka, wave amplitudes can be much bigger in pipes than on flat plates). When the above results are extended to cylindrical geometry, it could provide a more rigorous theoretical basis for our correlation. This extension will be pursued in future work.

We also compare our correlation with related experimental results in pipes and capillaries. Jayawardena et al. (1997) found that the annular-slug transition for gas-liquid two-phase flows in pipes in microgravity is correlated by

$$Re_{LS} = 0.215\times 10^{-3} Su^{2/3} Re_{GS} \quad (Su < 10^6). \qquad (12)$$

Comparing Eq. 12 with Eq. 1c, we see that the exponent on the Suratman number is the same for both cases. In normal gravity, the driving force for the liquid film is the gravity force, which is represented by the Galileo number. In microgravity, the driving force for the liquid film is the pressure gradient in the gas phase, which is represented by the gas Reynolds number. Thus, Eq. 1c and Eq. 12 show that one important parameter that determines the slug-annular transition in both normal and microgravity is the Suratman number.

The experimental results in Table 2 were combined with Eqs. 4 and 5 to determine the dimensionless flat film thickness (h_0/R) at occlusion, as well as the liquid fraction (A_L/A) in the pipe. The liquid fraction A_L/A in the pipe is defined as

$$\frac{A_L}{A} = 4\left(\frac{h_0}{D} - \frac{h_0^2}{D^2}\right). \qquad (13)$$

We note that the liquid fraction at the annular-slug transition varies from 0.4 to 0.7. This number should be compared with the empirical transition criterion ($A_L/A = 0.35$) suggested by Barnea et al. (1982) for cocurrent gas-liquid downflow in vertical pipes. The experimental results reported here clearly show that the liquid fraction at occlusion is higher than 0.35, at least in the laminar regime covered by our experiments ($Re_{LS} < 200$).

Figure 6 shows a plot of the dimensionless film thickness at occlusion as a function of the Capillary number for experiments conducted in a 0.5 in. diameter tube. Within the range of the data, the plot gives a straight line on a log-log scale with the following correlation

$$\frac{h_0}{R} = 0.73\,Ca^{3/8}. \qquad (14)$$

This relation may be compared with the empirical correlation obtained by Fairbrother and Stubbs (1935) for the thickness of the annular film in a capillary tube, which is initially filled with the liquid, and gas (or gas bubble) is blown through the tube. The empirical relation of Fairbrother and Stubbs and the experimental data of Goldsmith and Mason (1963) for the flow of large bubbles through horizontal capillary tubes gave the correlation

$$\frac{h_0}{R} = 0.5\,Ca^{1/2}, \qquad (15)$$

where the Capillary number is defined based on the gas velocity. Comparison of Eqs. 14 and 15 shows that, while the exponent on Ca is smaller in Eq. 14, the numerical value of the scaled film thickness at occlusion for a 0.5 in. diameter tube is about twice that predicted by Eq. 15.

Bretherton (1961) carried out an analysis on the same problem based on the planar lubrication theory and gave an analytical approximation for the scale film thickness

$$\frac{2h_0}{R} - \left(\frac{h_0}{R}\right)^2 \approx 1.29(3\,Ca)^{2/3}. \qquad (16)$$

Middleman (1995) eliminated the second term on the left-hand side of Eq. 16 and verified the validity of Brethertons theory for Capillary numbers in the range from 10^{-4} to 10^{-2} using the data reported by Taylor (1961), Bretherton (1961), and Schwartz et al., (1986). When the second term is neglected, Eq. 16 simplifies to

$$\frac{h_0}{R} = 1.4\,Ca^{2/3}. \qquad (17)$$

We found that Eq. 17 gave a very good agreement with our scaled film thickness in a 0.5 in. tube for Capillary numbers in the range of 0.05 to 0.1 (Table 3), even though with a different constant and exponent on Ca (Eqs. 14 and 17). Since

Table 3. Comparison of Scaled Film Thickness for 0.5 in. (12.7-mm) Tube with Capillaries

Ca	h_0/R (Eq. 14)	h_0/R (Eq. 15)	h_0/R (Eq. 17)
0.100	0.308	0.158	0.302
0.089	0.294	0.149	0.279
0.074	0.276	0.136	0.248
0.046	0.229	0.107	0.179
0.068	0.266	0.130	0.232
0.092	0.298	0.152	0.285
0.171	0.376	0.207	0.431
0.196	0.397	0.222	0.473
0.277	0.451	0.263	0.595
0.093	0.299	0.152	0.286
0.087	0.293	0.148	0.276
0.073	0.274	0.135	0.245

the Capillary number in our experiments is larger than 0.01, this agreement may be fortuitous.

The experimental observations of Taylor show that for *Ca* greater than 2, h_0/R becomes independent of *Ca* and approaches a value of 0.33 for residual annular film in capillaries. For falling film in vertical pipe, this is not the case. Table 3 shows that for a very viscous solution, the scaled film thickness can be as large as 0.45.

A final comparison that we make is with the experimental data of Gauglitz and Radke (1988) on the formation and breakup of liquid bridges in capillaries. Experimental data of these authors show that liquid bridges are formed in capillaries when h_0/R exceeds 0.09. In the case of falling films in a 0.5 in. vertical pipe, the smallest scaled film thickness at occlusion was found to be 0.23. Based on these comparisons, it appears that the wave occlusion problem in vertical pipes is qualitatively different from that of liquid bridge formation in capillaries.

Acknowledgment

This work was supported by grants from the NASA Glenn Research Center (NAG3-1840) and the Graduate Student Researchers Program (GSRP) fellowship (NGT3-52356) to Eric K. Dao.

Literature Cited

Barnea, D., O. Shoham, and Y. Taitel, ''Flow Pattern Transitions for Vertical Downward Two-Phase Flow,'' *Chem. Eng. Sci.*, **37**, 741 (1982).

Bretherton, F. P., ''The Motion of Long Bubbles in Tubes,'' *J. Fluid Mech.*, **10**, 166 (1961).

CRC Handbook of Chemistry and Physics, CRC Press, Cleveland, OH (1978).

Dukler, A. E., ''The Role of Waves in Two Phase Flow: Some New Understandings,'' *Chem. Eng. Edu.*, 108 (1977—1978).

Dukler, A. E., and Y. Taitel, ''Flow Pattern Transitions in Gas-Liquid Systems: Measurement and Modeling,'' *Multiphase Sci. and Technol.*, **V2**, 1 (1986).

Fairbrother, F., and A. E. Stubbs, ''Studies in Electroendosmosis. Part VI. The Bubble-Tube Method of Measurement,'' *J. Chem. Soc.*, **1**, 527 (1935).

Gauglitz, P. A., and C. J. Radke, ''An Extended Evolution Equation for Liquid Film Breakup in Cylindrical Capillaries,'' *Chem. Eng. Sci.*, **43**, 1457 (1988).

Goldsmith, H. L., and S. G. Mason, ''The Flow of Suspensions through Tubes II. Single Large Bubbles,'' *J. Colloid Sci.*, **18**, 237 (1963).

Hewitt, G. F., and P. B. Whalley, ''Vertical Annular Two Phase Flow,'' *Multiphase Sci. and Technol.*, **V4**, 103 (1989).

Jayawardena, S. S., V. Balakotaiah, and L. C. Witte, ''Flow Pattern Transition Maps for Microgravity Two-Phase Flows,'' *AIChE J.*, **43**, 1637 (1997).

Middleman, S., *Modeling Axisymmetric Flows, Dynamics of Films, Jets, and Drops*, Academic Press, San Diego, CA, p. 57 (1995).

Nguyen, L. T., and V. Balakotaiah, ''Modeling and Experimental Studies of Wave Evolution on Free Falling Viscous Films,'' *Phys. Fluids*, (Sept. 2000).

Schwartz, L. W., H. M. Princen, and A. D. Kiss, ''On the Motion of Bubbles in Capillary Tubes,'' *J. Fluid Mech.*, **172** 259 (1986).

Taylor, G. I., ''Deposition of a Viscous Fluid on the Wall of a Tube,'' *J. Fluid Mech.*, **10**, 161 (1961).

Manuscript received June 7, 1999, and revision received Jan. 4, 2000.